ORIGINAL ARTICLE

Development and Control of Novel Vibration Isolation Platform

Meng-Shiun Tsai*, Yann-Shuoh Sun, and Zhong-Shian Wu

Department of Mechanical Engineering, National Chung-Cheng University, Taiwan

(**Received** 30 June 2013, **Accepted** 2 September 2013; **Published on line** 1 December 2013)

*Corresponding author: imetsai@ccu.edu.tw

DOI: 10.5875/ausmt.v3i4.213

Abstract: A vibration isolation platform designed to attenuate high frequency vibration is proposed consisting of an active layer driven by a piezoelectric actuator and a passive layer. The proposed platform can achieve vibration isolation both in the vertical and horizontal directions. The dynamic behavior of the system is analyzed by deriving the equations of motions using the Lagrangian approach. System identifications are performed to validate the plant dynamics. The robust H_∞ controller is adopted to design the controller with consideration of payload uncertainties. Experimental results show that the control can reduce vibrations by an average of 10dB within a frequency range of 15-40Hz.

Keywords: Vibration isolation; pendulum structure; active-passive; H_∞ controller

Introduction

The importance of vibration isolation is increasing as manufacturing technology moves toward the nanoscale. Passive, active and active-passive techniques have been developed to protect high precision equipment from ground disturbance. Passive vibration isolation systems use an oil channel, pneumatic device or damping layer to reduce the transmission of seismic vibration. The passive approach uses a low first resonance frequency with a high mass and low stiffness, such as an optical table. The frequency response between the magnitude of the payload and ground disturbance could have a 20dB/decade attenuation after passing the first natural frequency. However the passive isolators could result in the vibrations around the resonance being amplified rather than isolated. Using a high damping ratio can reduce the vibration around the resonance, but this could reduce the attenuation rate after the resonance. Applying active controls can provide more vibration attenuation around the resonance. Aside from the critical passive design problem, passive systems can only handle light payloads due to the low stiffness design [1]. The semi-active system was proposed to control stiffness and damping, using a damper design proposed by [2] or the Magnetorheological damper [3].

During the past two decades, active and active-passive systems using piezoelectric actuators have been widely studied [4, 5]. The active-passive system generally consists of an active layer and a passive layer to achieve advantages such as stability, energy savings, and robustness. Many control techniques have been proposed including classical control [6, 7]. Optimal LQG control [8] adaptive control [9], and neural networks [10]. ecently, six degree of freedom systems such as the Stewart platform [11] have been proposed. The cross coupling effects between each leg were investigated [8, 12] using either the singular value decomposition method or modal decompositions.

Although many designs have been proposed to achieve active-passive vibration isolation systems, such designs were only focused on reducing the transmissibility in the vertical direction without considering the horizontal direction. This paper proposes a novel pendulum-typed system consisting of three

active cables embedded with piezoelectric actuators. The proposed design can passively attenuate horizontal vibrations while its active actions attenuate vertical vibrations. Theoretical modeling and experiments are conducted to validate the design concept. A robust controller based on H∞ theory is then proposed to deal with payload uncertainties. Experiments are conducted to validate the controller performance.

Equations of Vertical and Horizontal Motion

Figure 1 illustrates the interior design of the pendulum-type vibration isolation system. The system comprises three cables connecting the outer case and intermediate (center) mass. The piezoelectric actuator and accelerometer are embedded in the intermediate mass to form the active layer. On top of the intermediate mass, an isolation pad and payload disk form the passive layer. To test the isolation performance, the system is set on a marble table. The proposed system can provide active control for low-frequency vibrations and a passive attenuation of high-frequency vibrations due to the low first natural frequency of the pendulum. The closed loop control picks up the vibration signal from the accelerometer and then drives the piezoelectric actuators based on the designed control algorithm. The low frequency vibration transmissibility is first reduced by the first active layer. The high frequency vibrations can be then further reduced by the passive layer. Because the vibration around the resonance cannot be reduced passively, the active action can provide the isolation around this region to achieve the advantages of both the active and passive effects.

Dynamic Equation in the Vertical Direction

To derive the dynamic model, the schematic of the vibration system can be represented by the lumped parameter system in the vertical direction as shown in Figure 2.

Meng-Shiun Tsai received his PhD in mechanical engineering from Pennsylvania State University in 1998. He is currently Professor of Mechanical Engineering at National Chung-Cheng University, Taiwan. His research interests are focused on motion controls, piezoelectric-based smart structures, SAW devices, ultrasonic motors, and machine tools. He is a member of the National Honor Society of Phi Kappa Phi.

Yann-Shuoh Sun is a PhD candidate in Mechanical Engineering at the National Cheng Kung University, Taiwan. Since 1995, he has been with the Industrial Technology Research Institute, Taiwan, where he is currently a Researcher in the Robotics System Integration Department of the Intelligent Robotics Technology Division. His research interests are focused on vibration testing and control, modal testing and analysis.

Zhong-Shian Wu received his M.S. in Electrical Engineering from National Chung Cheng University in 2011.

Generally, the force of the piezoelectric actuator can be represented as [13]

$$F_a = -J_c V + k_a \Delta, \quad (1)$$

where k_a is the stiffness of the piezoelectric actuators, J_c is the driving coefficient, and ΔX is the displacement of the actuators .

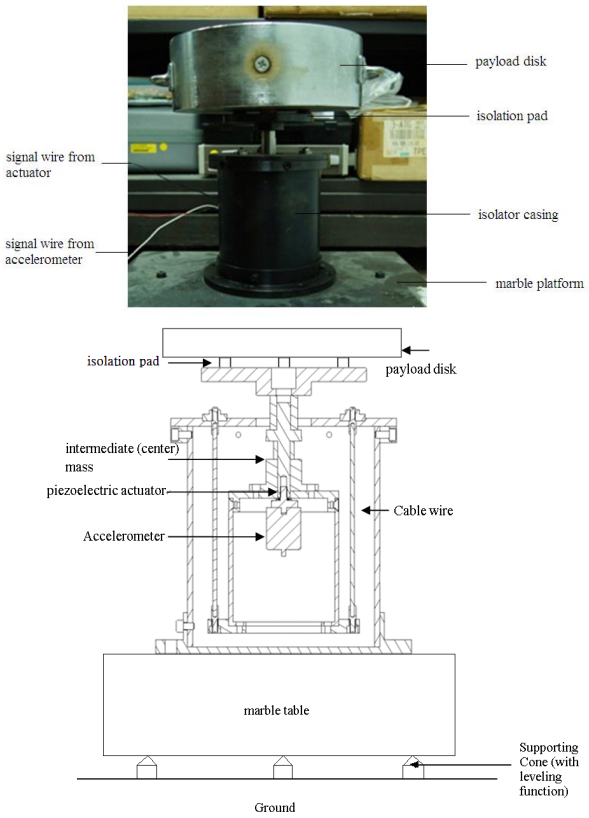

Figure 1. Schematic illustrations of vibration isolation platform.

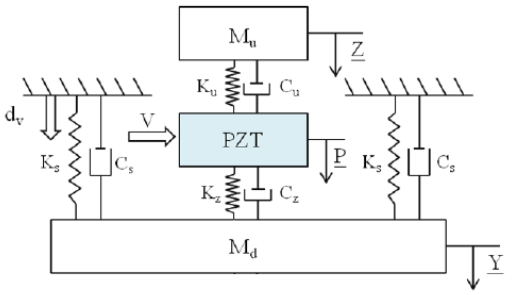

Figure 2. Lumped parameter system representing the vibration isolation system in the vertical direction.

The dynamic equation can be derived by using the energy method with the Lagrangian approach. First, the kinetic energy T_a, potential energy V_a and virtual work in the vertical direction shown in Figure 2 can be expressed as:

$$T_a = \frac{1}{2} M_u \dot{Z}^2 + \frac{1}{2} M_d \dot{Y}^2, \quad (2)$$

$$V_a = \frac{1}{2}K_u(P-Z)^2 + \frac{1}{2}K_z(Y-P)^2 + \frac{1}{2}K_s(Y-dv)^2, \quad (3)$$

$$\begin{aligned}\delta W = F\delta z - C_u(\dot{P}-\dot{Z})\delta(P-Z) - \\ C_z(\dot{Y}-\dot{P})\delta(Y-P) - C_s(\dot{Y}-\dot{dv})\delta(Y-dv)\end{aligned}. \quad (4)$$

By applying the Lagrange formulation given in Eq. (5), the dynamic equations can be formulated as Eq. (6).

$$\frac{\mathrm{d}}{\mathrm{dt}}\frac{\partial L}{\partial \dot{q}_i} - \frac{\partial L}{\partial q} = Q_i, \quad (5)$$

$$\begin{bmatrix} M_u & 0 & 0 \\ 0 & M_d & 0 \\ 0 & 0 & 0 \end{bmatrix}\begin{bmatrix} \ddot{Z} \\ \ddot{Y} \\ \ddot{P} \end{bmatrix} + \begin{bmatrix} C_u & 0 & -C_u \\ 0 & C_z + C_s & -C_z \\ -C_u & -C_z & C_u + C_z \end{bmatrix}\begin{bmatrix} \dot{Z} \\ \dot{Y} \\ \dot{P} \end{bmatrix} + \begin{bmatrix} K_u & 0 & -K_u \\ 0 & K_z + K_s & -K_z \\ -K_u & -K_z & K_u + K_z \end{bmatrix}\begin{bmatrix} Z \\ Y \\ P \end{bmatrix} = \begin{bmatrix} 0 \\ C_s \\ 0 \end{bmatrix}\dot{d}_v + \begin{bmatrix} 0 \\ K_s \\ 0 \end{bmatrix} d_v \quad (6)$$

Here, Mu and Md respectively represent the upper and intermediate masses, while dv is the vertical disturbance displacement.

Dynamic Equation in the Horizontal Direction

The horizontal dynamic equation can be represented by the simplified lumped parameter system as shown in Figure 3. Here dh is the horizontal disturbance displacement, X_T is the corresponding displacement of the upper mass in the horizontal direction, and θ is the angle of the cables with respect to the vertical direction.

Based on the assumption that the rotational angle is small and the elongation of the cable can be negligible, the kinetic energy T_h, potential energy V_h and virtual work in the horizontal direction can be represented as:

$$T_h = \frac{1}{2}M_u\dot{X}^2 + \frac{1}{2}M_d\left(L_W\frac{d\sin\theta_w}{dt} + \dot{d}_h\right)^2, \quad (7)$$

$$V_h = \frac{1}{2}K_{uh}(X_T - L_W\sin\theta_w - d_h)^2 + g(M_u + M_d)(L_W - L_W\sin\theta_w), \quad (8)$$

$$\begin{aligned}\delta W_h = C_{uh}\left(\dot{X}_T - L_W\frac{d\sin\theta_w}{dt} - \dot{d}_h\right)\delta\left(X_T - L_W\sin\theta_w - d_h\right) \\ + C_{dh}\left(L_W\frac{d\sin\theta_w}{dt}\right)\delta\left(L_W\sin\theta_w\right)\end{aligned}. \quad (9)$$

By applying the Lagrange equation, the dynamic equations in the horizontal direction are expressed as:

$$\begin{bmatrix} M_u & 0 \\ 0 & (M_u + M_d)L^2_W \end{bmatrix}\begin{bmatrix} \ddot{X}_T \\ \ddot{\theta}_W \end{bmatrix} + \begin{bmatrix} C_{uh} & -C_{uh}L_W \\ -C_{uh}L_W & (C_{uh} + C_{dh})L^2_W \end{bmatrix}\begin{bmatrix} \dot{X}_T \\ \dot{\theta}_W \end{bmatrix} + \begin{bmatrix} K_{uh} & -K_{uh}L_W \\ -K_{uh}L_W & (M_u + M_d)L_W g + K_{uh}L^2_W \end{bmatrix}\begin{bmatrix} X_T \\ \theta_W \end{bmatrix} = \begin{bmatrix} 1 \\ 0 \end{bmatrix}F + \begin{bmatrix} 0 \\ -(M_u + M_d)L_W \end{bmatrix}\ddot{d}_h + \begin{bmatrix} C_{uh} \\ -C_{uh}L_W \end{bmatrix}\dot{d}_h + \begin{bmatrix} K_{uh} \\ -K_{uh}L_W \end{bmatrix} d_h \quad (10)$$

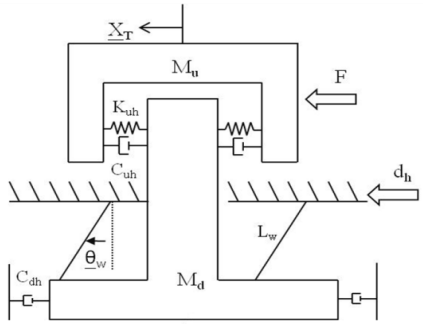

Figure 3. Lumped parameter representation of vibration isolation system in horizontal direction.

Experimental Validation and Analysis of the Dynamic Model

This section presents the validation and analysis of the dynamic model by comparing the experimental and simulation results. The frequency response of the vertical model can be obtained by applying a chirp sine signal to the piezoelectric actuator and obtaining the output signal from the accelerometers embedded in the intermediate mass using the dynamic signal analyzer HP35670A. Figure 4 shows the simulation and experimental results are in good agreement. Next, the model in the horizontal direction can be validated by hitting the upper mass with a hammer and then measuring the signal from the accelerometer mounted on the upper mass. The frequency response function between XT and F in Figure 3 is shown in Figure 5.

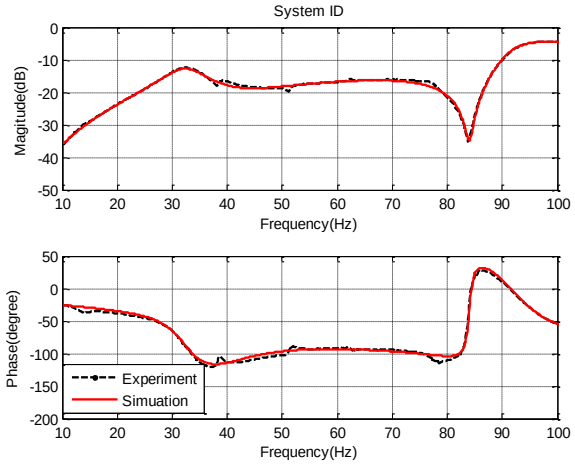

Figure 4. Simulation and experimental results for frequency response function in the vertical direction.

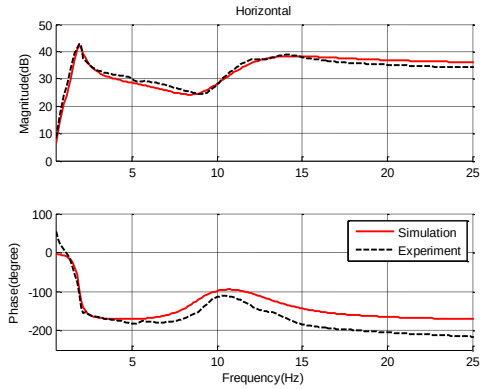

Figure 5. Simulation and experimental results for frequency response function in the horizontal direction.

Because the vibration in the horizontal direction should be attenuated passively, the frequency response function between the disturbance dh and XT is important for the evaluating the passive transmissibility, as shown in Figure 6. The results demonstrate that the pendulum causes low resonance at about 1.65Hz. After the first resonance the isolation become effective until the second resonance at about 12Hz. The second resonance is mainly caused by the passive isolation pad and the mass effect from the intermediate and upper mass. The horizontal disturbance can obtain an attenuation of at least 5 dB above 16.5Hz. Any disturbance consisting of a frequency above 20Hz can be reduced by more than 10 dB. The only tradeoff is that the input is amplified when the frequency is lower than 2 Hz, mainly due to the low damping of the pendulum system, but this can be solved by adding oil in the case. The oil provides a resistive force to the motion of the intermediate mass, thus increasing the damping force. The second approach is to attach another damper between the outer case and the intermediate mass. Both methods can increase the damping C_{dh} in Figure 3. However, as mentioned above, the passive control could amplify the resonance even with a high damping design. This drawback can be improved through the use of active controls.

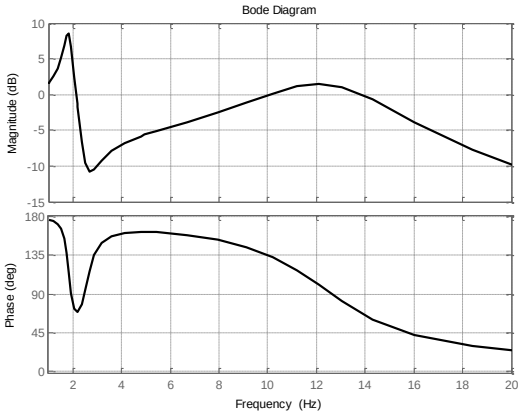

Figure 6 Simulation results for transmissibility in the horizontal direction.

Robust H∞ Control of the Platform

After obtaining the frequency response of the plant shown in Figure 4, the next step is to perform the active control for the isolation platform in the vertical direction. In real applications, the weight of the payload set on the vibration platform could vary significantly. To account for the payload uncertainty, this study adopts the robust H∞ control.

Figure 7 shows the block diagram used in designing the robust controller where d is the disturbance, P(s) is the plant, and K(s) is the controller. W1(s) and W2(s) are the performance weighting and uncertainty weighting functions, respectively. Here the multiplicative uncertainty model is used to describe the plant uncertainty under different payloads. As shown in Figure 7, the multiplicative uncertainty can be described as:

$$\Delta P(s) = \frac{P(s) - P_0(s)}{P_0(s)}. \tag{11}$$

The nominal plant P0(s) is defined as a payload equal to 50 Kg. One of the disturbed plant P(s) is set as a plant with a payload equal to 40 Kg. The other has a payload equal to 60 Kg. The weighting function $W_2(s)$ is chosen to cover the uncertainty of $\Delta P(s)$. As shown in Figure 8, the $\Delta P(s)$ of the frequency response functions for the plants with different payloads are measured and $W_2(s)$ is chosen to cover the uncertainty.

$$W_2(s) = \frac{4s + 450}{s + 400}. \tag{12}$$

The performance weighting function W1(s) is chosen as a low pass filter which weighs heavily at the target frequencies from 10Hz to 50Hz. The frequency responses of $W_1(s)$ are shown in Figure 9. After the weighting functions are selected, the block diagram in Figure 9 can be expressed in the form of the linear fractional transformation shown in Figure 10. Here, the augmented plant Pa is given as:

$$\begin{bmatrix} z_1 \\ z_2 \\ e \end{bmatrix} = \begin{bmatrix} -W_1 & -W_2 & -W_1 P \\ 0 & 0 & W_2 P \\ -1 & -1 & -P \end{bmatrix} \begin{bmatrix} d_1 \\ d_2 \\ u \end{bmatrix}, \tag{13}$$

and

$$\Delta = \begin{bmatrix} \delta_1 & 0 \\ 0 & \delta_m \end{bmatrix}. \tag{14}$$

$\delta 1$ and δm are 1x1 diagonal blocks reflecting the nominal performance and robust stability respectively. Δ is normalized as $\|\Delta\|_\infty < 1$. With the given augmented plant, the H∞ controller K(s) can be obtained easily by solving two Riccati equations [14, 15].

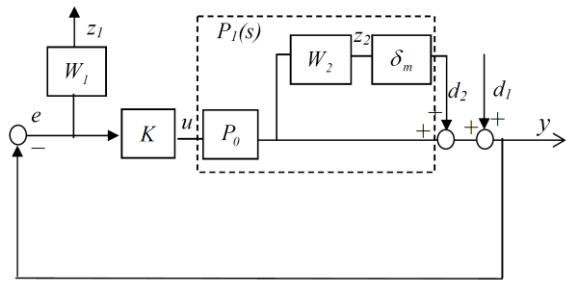

Figure 7. Block diagram of the controlled system with plant uncertainty.

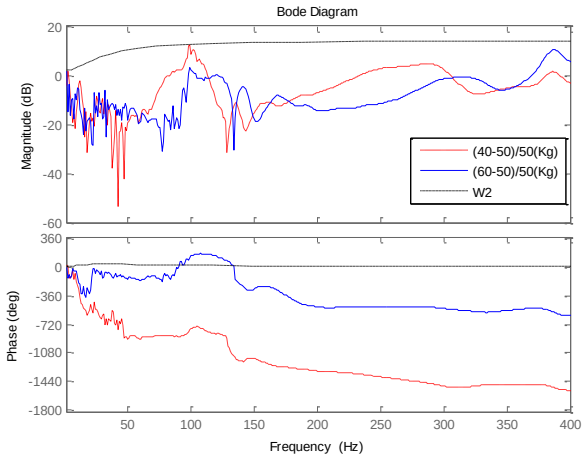

Figure 8. Frequency response of the plant uncertainty.

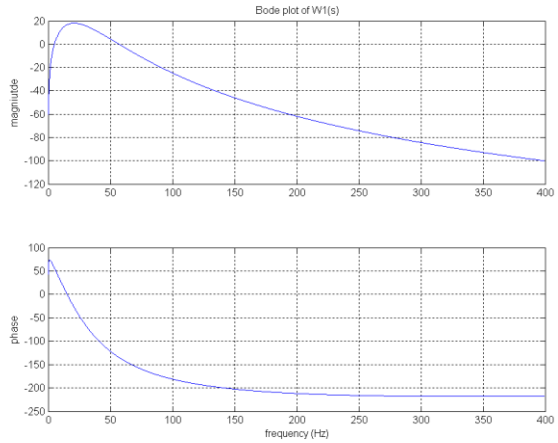

Figure 9. Frequency response functions of the weighting function *W1(s)*.

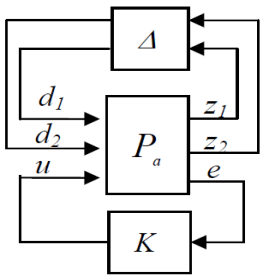

Figure 10. A linear fractional representation of the control system.

After designing the controller, experiments were conducted to validate system performance. From the performance weighting shown in Figure 9, it is found that higher weightings are set within a frequency range from 10 to 50 Hz. The controller is then implemented on a DSP-based controller with an A/D sampling equal to 1 KHz. The disturbance can be simulated by generating a chirp sine signal injected into the plant at a control voltage u, with results shown in Figure 11. The disturbance rejection achieved is about 10 dB within a frequency range of 10-45 Hz, with some spillovers within a frequency of 45-60 Hz. Since the high frequency disturbances can be attenuated by passive damping, future work will evaluate the design of a passive layer to reduce the spillover effect.

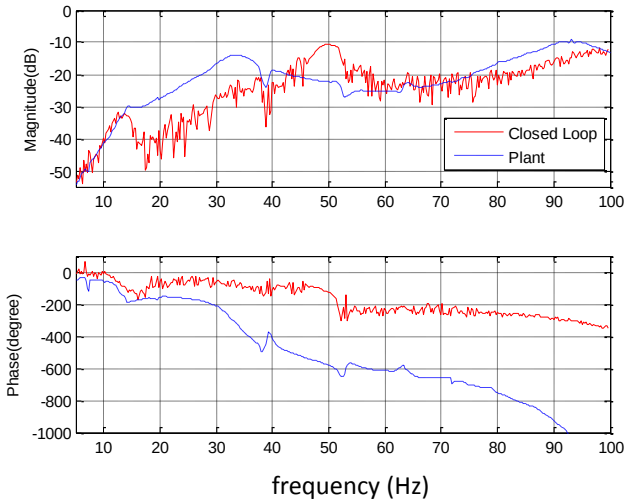

Figure 11. Comparison between the open loop and closed loop systems.

Conclusion

A novel active-passive vibration isolation platform is proposed where the active layer in the vertical direction consists of a pendulum structure and a piezoelectric actuator with accelerometer embedded in the intermediate mass. On top of the active layer, a passive layer is designed to attenuate high frequency vibration. The isolation effect in the horizontal direction is purely passive. With the aid of pendulum structure, the first natural frequency can be reduced to about 1.5 Hz which can help attenuate high frequency disturbances. To understand the dynamic behavior of the system, the motion equations in the vertical and horizontal directions are derived using the Lagrangian approach. Device performance is validated by experiments and is used as the basis for controller design. To account for payload uncertainty, the robust H_∞ controller is adopted. The uncertainty weighting function is determined to cover payloads ranging from 40 Kg to 60 Kg. Experimental results show that the active control can reduce the vibration by an average of 10dB within the frequency range from 15-40Hz.

Acknowledgement

The authors are grateful to the ROC Ministry of Economic Affairs for financial support provided under contract 101-EC-17-A-05-S1-189.

References

[1] S. S. Rao, *Mechanical vibrations*. Reading, Mass.: Addison-Wesley, 1990.

[2] D. Karnopp, M. J. Crosby, and R. A. Harwood, "Vibration control using semi-active force generators," *Journal of Engineering for Industry,* vol. 96, no. 2, pp. 619-626, 1974. doi: 10.1115/1.3438373

[3] A. L. Browne, E. Cook, W. Hu, and N. M. Wereley, "System and method for magnetorheological fluid damping utilizing porous media," US Patent 7874407, 2011.

[4] S. Sarai, M. Ikeda, and T. Miura, "Decentralized position and attitude control of a vibration isolation system," in *IEEE International Conference on Control Applications (CCA '01)*, 2001, pp. 1026-1030. doi: 10.1109/CCA.2001.974005

[5] M. S. Tsai, Y. S. Sun, and C. H. Liu, "Robust control of novel pendulum-type vibration isolation system," *Journal of Sound and Vibration,* vol. 330, no. 18–19, pp. 4384-4398, 2011. doi: 10.1016/j.jsv.2011.04.024

[6] L. A. Sievers and A. H. Von Flotow, "Comparison of two LQG-based methods for disturbance rejection," in *the 28th IEEE Conference onDecision and Control*, 1989, pp. 483-485 vol.481. doi: 10.1109/CDC.1989.70161

[7] A. M. Beard, D. W. Schubert, and A. H. von Flotow, "A practical product implementation of an active/passive vibration isolation system," *Active Control of Vibration and Noise,* vol. 75, pp. 485-492, ASME DE 1994.

[8] T. T. Hyde, "An experimental study of active vibration isolation," in *38th Structures, Structural Dynamics, and Materials Conference*, 1997, vol. 2, pp. 1763-1773. doi: 10.2514/6.1997-1354

[9] E. H. Anderson and J. P. How, "Active vibration isolation using adaptive feedforward control," in *American Control Conference*, 1997, vol. 3, pp. 1783-1788. doi: 10.1109/ACC.1997.610892

[10] K. G. Ahn, H. J. Pahk, M. Y. Jung, and D. W. Cho, "A hybrid-type active vibration isolation system using neural networks," *Journal of Sound and Vibration,* vol. 192, no. 4, pp. 793-805, 1996. doi: 10.1006/jsvi.1996.0218

[11] Z. Han, C. Joshi, and A. Mavanur, "Active vibration isolation system," US Patent 20030168295, 2003.

[12] P. Heiland and P. A. Kropp, "Control of an active vibration isolation system," US Patent 7489987, 2009.

[13] "IEEE standard on piezoelectricity," *ANSI/IEEE Std 176-1987,* 1988. doi: 10.1109/IEEESTD.1988.79638

[14] M. S. Tsai and J. S. Chen, "Robust tracking control of a piezoactuator using a new approximate hysteresis model," *Journal of Dynamic Systems, Measurement, and Control,* vol. 125, no. 1, pp. 96-102, 2003. doi: 10.1115/1.1540114

[15] J. C. Doyle, B. A. Francis, and A. Tannenbaum, *Feedback control theory*. New York: Maxwell Macmillan, 1992.

Table 1. Parameters of vibration isolation module in horizontal and vertical directions.

M_u	50 Kg
M_d	2.54
K_u	2 N / m
K_{uh}	0.57N/ m
K_z	10 N / m
K_s	1 N/ m
C_u	1200 N.sec / m
C_{uh}	300 N.sec / m
C_z	700 N.sec / m
C_s	700 N.sec / m
C_{dh}	90 N.sec / m
J_c	0.1 N / V
c_h	58 N sec / m
L_w	0.0375 m